The effects of variable viscosity on the decay of homogeneous isotropic turbulence.

Benoît-Joseph Gréa, Jérôme Griffond, Alan Burlot

The effects of variable viscosity on the decay of homogeneous isotropic turbulence

Benoît-Joseph Gréa, Jérôme Griffond, and Alan Burlot

Citation: Physics of Fluids (1994-present) **26**, 035104 (2014); doi: 10.1063/1.4867893
View online: http://dx.doi.org/10.1063/1.4867893
View Table of Contents: http://scitation.aip.org/content/aip/journal/pof2/26/3?ver=pdfcov
Published by the AIP Publishing

PHYSICS OF FLUIDS **26**, 035104 (2014)

The effects of variable viscosity on the decay of homogeneous isotropic turbulence

Benoît-Joseph Gréa,[a] Jérôme Griffond, and Alan Burlot
CEA, DAM, DIF, F-91297 Arpajon, France

(Received 18 November 2013; accepted 24 February 2014; published online 13 March 2014)

In this paper, we investigate the decay of incompressible homogeneous isotropic turbulence in a variable viscosity fluid. The viscosity coefficient is assumed to depend linearly on a scalar, representing either a temperature or a concentration, and obeying a simple advection-diffusion equation. At high Reynolds numbers, Direct Numerical Simulations (DNS) allow us to confirm the validity of Taylor's postulate that the dissipation is independent from the viscosity and its fluctuations. At low Reynolds numbers, we report the presence of extra energy at small scales due to these variable viscosity effects. This implies that the turbulent kinetic energy decreases less rapidly as a function of time in variable viscosity fluids. In order to explain this phenomenon and quantify its importance on the turbulent flow, we propose a statistical approach based on an eddy-damped quasi-normal Markovian (EDQNM) spectral closure which takes into account the nonlinearity introduced by variable viscosity. It is shown that this latter additional term is of constant sign in the energy spectrum equation and reduces the dissipation of the flow as observed. Also, by assuming the dominance of distant interactions between wave numbers, we can propose a simple formula expressing that variable viscosity effects lead to an effective reduction of the mean viscosity proportional to the variance of viscosity fluctuations. [http://dx.doi.org/10.1063/1.4867893]

I. INTRODUCTION

In many turbulent flows, the dependence of the viscosity coefficient on temperature or mix composition can be large and may significantly impact the dynamics. For instance, considering turbulent convection in the earth's mantle, the viscosity decreases with temperature giving rise to steep gradients. The transition to a turbulent convective regime is sensitive to this effect,[1] and phenomena such as viscous sublayers or "stagnant lids"[2–4] may appear at a later stage. In contrast, for plasmas in kinetic regime, viscosity rapidly increases with temperature.[5] This may alter the growth rates of hydrodynamic instabilities like Rayleigh-Taylor[6] which determine the yield of inertial confinement fusion (ICF) capsules.[7] Another case of importance is the mixing between two fluids of different viscosities induced by the Kelvin-Helmholtz instability. Such situations occur in turbulent jets, and the concentration-dependent viscosity may modify the entrainment mechanism during the transition to turbulence.[8] A strong gradient of viscosity may also relaminarize mixing zones at late stage in magma fountains.[9] Still, the precise role of variable viscosity is not completely understood as it is entangled with the complex features of inhomogeneous and anisotropic turbulent flows.

Therefore, to identify the different mechanisms acting in turbulent flows with variable viscosity, it seems desirable to focus on simpler configurations. In this work, we explore the interplay between variable viscosity and incompressible unforced homogeneous isotropic turbulence. In our idealized approach, the viscosity coefficient depends linearly on a scalar and is free to fluctuate around a constant mean value. At high Reynolds number (R_e), inhomogeneous configurations due to a mean viscosity gradient have been investigated numerically by Lee *et al.*[10]. In this latter study, the

[a]Electronic mail: benoit-joseph.grea@cea.fr

influence of the variable viscosity terms on the dissipation was found negligible. This appears to support the relevance of Taylor's postulate,[11] i.e., the independence of dissipation from the viscosity. From a theoretical point of view, however, this conclusion should be examined more extensively since variable viscosity effects produce additional terms in the equation for dissipation. This may unbalance the equilibrium between vortex stretching production and enstrophy destruction,[12,13] both terms growing as $R_e^{1/2}$. It seems, but remains unexplained, that the fluctuations of velocity are able to adapt themselves quick enough to steep viscosity gradients. As a consequence at high Reynolds numbers, the variable viscosity term does not affect the decay of turbulence which is driven by the large scales only as in a constant viscosity fluid.[14,15]

In this work, we would like to shed some new light on this phenomenon by proposing the idea that a flow with a variable viscosity has an effective Reynolds number which is higher than a flow with the same average but constant viscosity. This theory supports Taylor's postulate in the case of variable viscosity fluids. But as importantly, it explains that when finite Reynolds effects are observed, the variable viscosity effects slow down the decay of turbulence making constant and variable viscosity fluids to behave quite differently.

This paper is organized as follows. In Sec. II, we write the basic equations and highlight the particularities of freely decaying turbulence in a variable viscosity fluid. In Sec. III, several direct numerical simulations are presented in order to show the variable viscosity contributions. In Sec. IV, we propose a theoretical framework based on an Eddy-Damped Quasi-Normal Markovian (EDQNM) closure for the variable viscosity and we utilize it to quantify its effects.

II. GENERAL CONTEXT

In this section, the problem of decay of turbulence in a variable viscosity fluid is introduced. The system of equations is described together with the different notations used in this paper in Sec. II A. In Sec. II B, we write the equation for total kinetic energy and show that an additional term appears due to viscosity fluctuations.

A. Basic equations

We start from the incompressible Navier-Stokes equations for an homogeneous isotropic velocity field u_i. In this problem, the mean velocity of the fluid is assumed to equal zero, $\langle u_i \rangle = 0$. We note $\langle\rangle$ the ensemble averaging operator.

The total viscosity ν_{tot} can be decomposed into a mean viscosity noted ν ($= \langle \nu \rangle$) and a fluctuation $\nu' = \mathcal{V}c$ (with $\langle \nu' \rangle = 0$) as

$$\nu_{\text{tot}} = \nu + \mathcal{V}c, \tag{1}$$

where c is the scalar representing the temperature or the concentration fluctuations and $\mathcal{V}$ is a positive constant. In real systems, the viscosity dependency is not necessarily linear and may follow a much more complex relationship. Still, this idealized representation is relevant when the fluctuations of the scalar are small. This linear dependence is also convenient as it enables quasi-normal closures used later in this work.

Therefore, we obtain the following system of equations:

$$\partial_t u_i + u_j \partial_j u_i = -\partial_i p + \mathcal{V}\partial_j \left(c \partial_j u_i\right) + \nu \partial^2_{jj} u_i, \tag{2a}$$

$$\partial_i u_i = 0, \tag{2b}$$

$$\partial_t c + u_j \partial_j c = \kappa \partial^2_{jj} c. \tag{2c}$$

Equation (2a) is the equation for the velocity with p the reduced pressure (i.e., divided by the density). Equation (2b) gives the incompressibility condition and Eq. (2c) is the linear advection-diffusion equation for the scalar. We use Einstein's notations in the different equations.

In Eq. (2c), the coefficient κ appears, here taken constant, standing for conductivity or molecular diffusion. The ratio ν/κ defines thereafter the Prandtl number ($\mathcal{P}_r$) although it may refer to a Schmidt

number alike. This parameter is of importance in the problem. Indeed, at high $\mathcal{P}_r$, the variance of c is expected to maintain itself which should enhance variable viscosity effects in Eq. (2a).

Now we need to mention some properties of the scalar. Like the velocity and as already suggested, the scalar has a zero mean value, $\langle c \rangle = 0$. It becomes active in the momentum equation only through the variable viscosity term, which is statistically isotropic. We assume that initially, it is bounded, $c \in [-1, +1]$. It will stay in this interval, because it obeys a linear advection-diffusion equation (for incompressible flow). Also, note that $\mathcal{V} < \nu$ to ensure the positivity of the total viscosity ν_{tot}, at any time and everywhere in the flow.

B. The dissipation in a variable viscosity fluid

In this context, multiplying Eq. (2a) by u_i, averaging, using isotropy and homogeneity, we obtain the equation for the mean turbulent kinetic energy $E_T = \langle u_i u_i \rangle / 2$:

$$\frac{dE_T}{dt} = -\varepsilon, \text{ with } \varepsilon = \langle \nu_{\text{tot}} \partial_j u_i \partial_j u_i \rangle = \underbrace{\nu \langle \partial_j u_i \partial_j u_i \rangle}_{\varepsilon_a} + \underbrace{\mathcal{V} \langle c \partial_j u_i \partial_j u_i \rangle}_{\varepsilon_b}. \tag{3}$$

In Eq. (3), the dissipation ε is decomposed into two terms. The first one, ε_a, is the classical expression of dissipation for a flow with constant viscosity ν. The second term, ε_b, stems from viscosity fluctuations. While the sign of ε_a is clearly positive like that of ε, the sign of expression ε_b is undetermined. It can be negative as long as $\varepsilon > 0$ and turbulent kinetic energy decreases. Then, from Eq. (3) and the sign of ε_b, the following simple question arises: Does a fluid with constant viscosity $\overline{\nu}$ dissipate less than a variable viscosity fluid with the same mean viscosity $\langle \nu \rangle = \overline{\nu}$?

In addition, it is important to quantify the effect of term ε_b. In particular, we try to determine where it can be neglected or should be taken into account, and finally we derive a simple closure which may be implemented in a turbulence model.

III. DIRECT NUMERICAL SIMULATIONS

In order to study the problem proposed in Sec. II B, we performed several numerical simulations with variable viscosities at different Reynolds numbers. The domain of computation for the simulations is a cubic box of size 2π, with triply periodic boundary conditions. The total number of grid points is N^3, with N ranging from 256 to 2048.

A. Numerical method

The DNS of variable viscosity equations are based on a slight modification of a code addressing the classical uniform viscosity case.[16] This previous code uses a standard pseudospectral collocation method with phase-shift dealiasing (allowing to keep all Fourier modes with wavenumber k satisfying $k < \sqrt{2}N/3$) and a third order low-storage strong stability preserving Runge-Kutta scheme for time advancing. Accurate integration of viscous and diffusion terms is obtained by including the corresponding exponential damping term into each Fourier component.

The modification for computing the variable viscosity case is based on the splitting of the viscous term in two contributions $\partial_j[\nu_{\text{tot}} \partial_j u_i] = \partial_j[\nu_0 \partial_j u_i] + \partial_j[(\nu_{\text{tot}} - \nu_0)\partial_j u_i]$ where ν_0 is a uniform viscosity chosen lower or equal to the minimum value of viscosity in the flow ν_{min}, in order that the fluctuating viscosity $(\nu_{\text{tot}} - \nu_0)$ remains positive everywhere. The contribution of the uniform viscosity ν_0 is accounted for as usual in the standard part of the code whereas that of the fluctuating viscosity $(\nu_{\text{tot}} - \nu_0)$ is accounted for in an additional intermediate step before projection over divergence-free velocity fields. That additional step amounts to solve $\partial_t u_i = \partial_j[(\nu_{\text{tot}} - \nu_0)\partial_j u_i]$. For the sake of robustness, it is performed in the physical space with central finite difference approximations. Directional splitting is used with full implication in each direction requiring the resolution of three-diagonal or penta-diagonal periodic systems to get second or fourth order spatial accuracy. To enforce the positivity of the matrices of the systems to be solved, we introduce new constraints on the time-step which become stringent when the maximum of $|\nu_{\text{tot}} - \nu_0|$ grows.

TABLE I. Characteristics of the different numerical simulations of homogeneous isotropic turbulence with constant or variable viscosity considered in this work.

Name	Resolution	ν	$\nu_{\min}$	$\nu_{\max}$	$\frac{\langle\nu'\nu'\rangle}{\nu^2}(t=0)$	$\mathcal{P}_r$	R_e	$E_T(t=0)$
SA0	256^3	0.5	0.5	0.5	0	1	0.17	0.75
SA1	256^3	0.5	0.01	0.99	0.71	1	0.17	0.75
SA2	256^3	0.5	0.01	0.99	0.31	50	0.17	0.75
SA3	256^3	0.5	0.01	0.99	0.71	50	0.17	0.75
SB0	512^3	0.05	0.05	0.05	0	2.5	1.7	0.75
SB1	512^3	0.05	0.001	0.099	0.19	2.5	1.7	0.75
SB2	512^3	0.05	0.001	0.099	0.64	2.5	1.7	0.75
SB3	512^3	0.05	0.001	0.099	0.81	2.5	1.7	0.75
SC0	1024^3	0.005	0.005	0.005	0	2.5	17.6	0.75
SC1	1024^3	0.005	0.001	0.009	0.48	2.5	17.6	0.75
SD0	1024^3	0.0005	0.0005	0.0005	0	2.5	176	0.75
SD1	1024^3	0.0005	0.0001	0.0009	0.47	2.5	176	0.75
SE0	2048^3	0.0001	0.0001	0.0001	0	1	866	0.75
SE1	2048^3	0.0001	0.00005	0.00015	0.19	1	866	0.75

We have run different tests to study the influence of the spatial order for the variable viscosity term and the choice for ν_0 (generally taken as $\nu_{\min}$). We have checked that the different options in the numerical method do not modify the results of the simulations presented here.

B. Presentation of the simulations

The characteristics of the different simulations are displayed in Table I. Globally, we explore the effects of variable viscosity through a large range of Reynolds numbers, different initial variances of viscosity and to a lesser extent, several values of Prandtl numbers. The simulations are grouped into 5 categories corresponding to their initial Reynolds number which is based on the mean viscosity ν, a characteristic length based on the peak of initial spectra and the square root of the initial kinetic energy injected in the system. Thus, we use the following expression for the Reynolds number as considered for instance in Ref. 17 for freely decaying turbulence, $Re = E_T^{1/2}(0)/k_{peak}\nu$. From this definition, the different simulations SA, SB, SC, SD, and SE have respectively $Re = 0.17,\ 1.7,\ 17,\ 170,$ and 866.

The initial energy spectra are of the von Karman type $E(k, t=0) \propto k^4 \exp[-2(k/k_{peak})^2]$ with a maximum located at $k_{peak} = 10$. This value is a compromise between having a turbulent flow and minimizing the effects of confinement due to the finite size of the domain (as well as ensuring statistical convergence). In this work, we focus only on comparisons between constant and variable viscosity fluids. We do not intend to provide the decay rates of turbulence as mainly driven by the large scales. We just recall that the final decay of turbulence in our case evolves as $t^{-5/2}$ as shown by Ref. 14 for k^4 infrared spectra. The differences between constant and variable viscosity configurations are expected to appear at large wavenumbers. For this reason, we tolerate slight confinement effects which on the counterpart allows values of k_{peak} smaller than 80 chosen by Ref. 17 for instance and the exploration of higher Reynolds numbers. In addition, the amplitudes of initial spectra are related to their initial kinetic energy as $E_T = \int_0^{+\infty} E(k)dk$, set to 0.75 in all the simulations.

The initial scalar spectra $E_{cc}(k, t=0)$ are taken proportional to the initial energy spectra $E(k, t=0)$ such that they are also of the von Karman type with $k_{peak} = 10$. It is important to stress that the initial velocity and scalar fields are not correlated in our simulations, $\langle u_i c\rangle = 0$. The amplitudes of the scalar spectra are determined by the initial variance of viscosity $\langle\nu'\nu'\rangle$ with

$$\langle\nu'\nu'\rangle = \mathcal{V}^2\langle cc\rangle = 2\mathcal{V}^2\int_0^{+\infty} E_{cc}(k)dk. \tag{4}$$

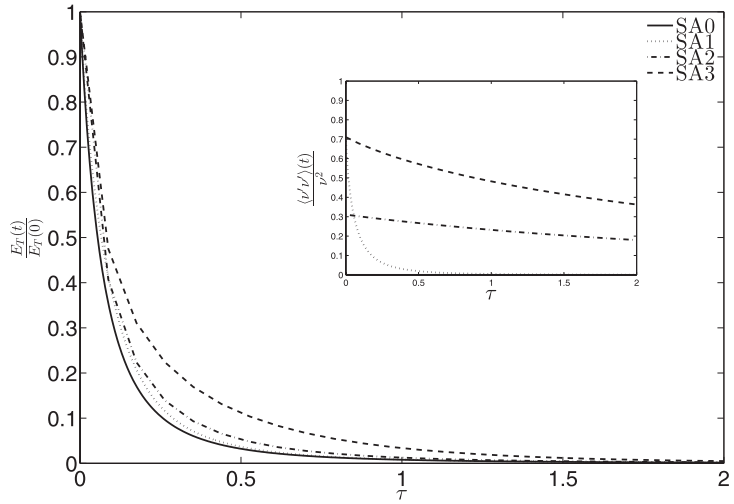

FIG. 1. Evolution of turbulent kinetic energy as a function of time for the simulations SA presented in Table I. Inset: Evolution of the variance of viscosity fluctuations as a function of time.

In addition, the constant $\mathcal{V}$ is obtained from the initial maximum and minimum of viscosity specified in Table I by the relation $\mathcal{V} = (\nu_{\max} - \nu_{\min})/2$. When the variance $\langle \nu'\nu' \rangle$ is small compared to ν^2, the initial distribution of viscosity is centred around ν. However, for higher values and due to the fact that in the simulations the viscosity is bounded to an interval, $\nu_{\text{tot}} \in [\nu_{\min}\ \nu_{\max}]$, there is an accumulation of viscosity values around extrema tending to an initial bimodal distribution (corresponding to $\langle \nu'\nu' \rangle / \nu^2 = (\nu_{\max} - \nu_{\min})^2/(\nu_{\max} + \nu_{\min})^2$). Of course, this distribution may be smoothed at later times by diffusion. The ratio between maximum and minimum of viscosity varies according to the simulations. It is close to 100 in SA and SB, 10 in SC and SD, and 3 in SE.

We impose the mesh size such that the smaller scales in the simulations with constant viscosity are well resolved, and we verify that the spatial step taken is smaller than the Kolmogorov scale.[18] It is more difficult to establish a similar criteria for the variable viscosity cases. Ideally, we would like to impose that an equivalent simulation with a constant viscosity taking the value $\nu_{\min}$ to be well resolved. In practice, however, this criteria is very stringent so it is not always completely satisfied at the very beginning of the simulations, in particular those at high Reynolds numbers (case SE). Due to the resolution of the scalar field, we have to restrict the Prandtl number parametric study to small Reynolds cases. The effect of high $\mathcal{P}_r$ is tested against simulations SA and SB only where it is possible to decrease κ while keeping small scales of the scalar field well resolved.

The different time evolutions of kinetic energy and viscosity variance of the DNS are presented in Figures 1–3 while the energy and scalar spectra at different times are shown in Figures 4–6. In the figures displayed, the dimensionless time τ is defined relatively to the initial eddy turnover time $1/E_T^{1/2}(0)k_{peak}$.

C. Observations

The aim of this section is to report different observations from the simulations concerning variable viscosity effects. For the moment, we postpone the theoretical interpretation of these results, they will be analysed later in the light of the statistical approach derived in Sec. IV.

The first point we would like to discuss is the sensitivity of variable viscosity effects to the Reynolds number. In fact, the influence of variable viscosity is clearly visible on the time evolution of kinetic energy and its dissipation at low Reynolds numbers (see cases SA-B in Figures 1 and 2). These effects tend to vanish at higher Reynolds numbers where the different curves of evolution of kinetic energy between constant and variable viscosity collapse (see cases SD and SE in Figure 3). These observations agrees with Taylor's hypothesis and with previous studies as for instance Ref. 10, already mentioned.

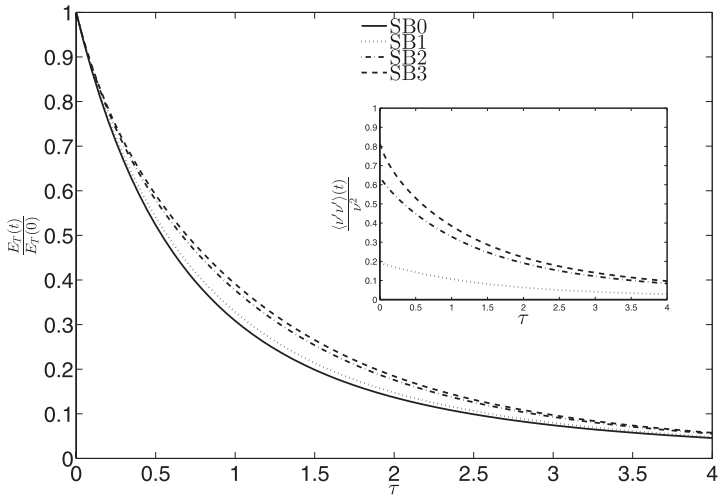

FIG. 2. Evolution of turbulent kinetic energy as a function of time for the simulations SB presented in Table I. Inset: Evolution of the variance of viscosity fluctuations as a function of time.

When looking at energy spectra, the differences between constant and variable viscosity simulations can be first perceived at very small scales (see Figures 4–6). In particular, it is striking that all variable viscosity spectra develop a larger tail. Nonetheless, this does not contribute much to the total kinetic energy on high Reynolds cases. It seems that variable viscosity fluids act as if they have an effective Reynolds number higher than their constant viscosity counterparts. In this work, we will try to develop and justify this point of view.

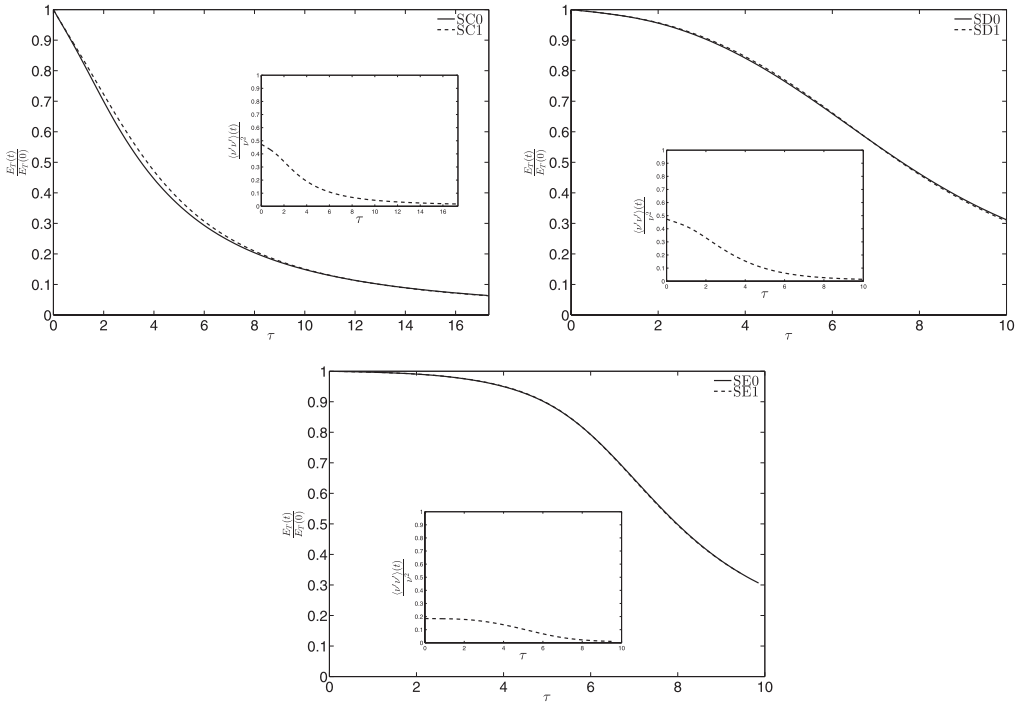

FIG. 3. Evolution of turbulent kinetic energy as a function of non-dimensionalized time τ for the simulations SC (top left), SD (top right), and SE (bottom) presented in Table I. Inset: Evolution of the variance of viscosity fluctuations as a function of τ.

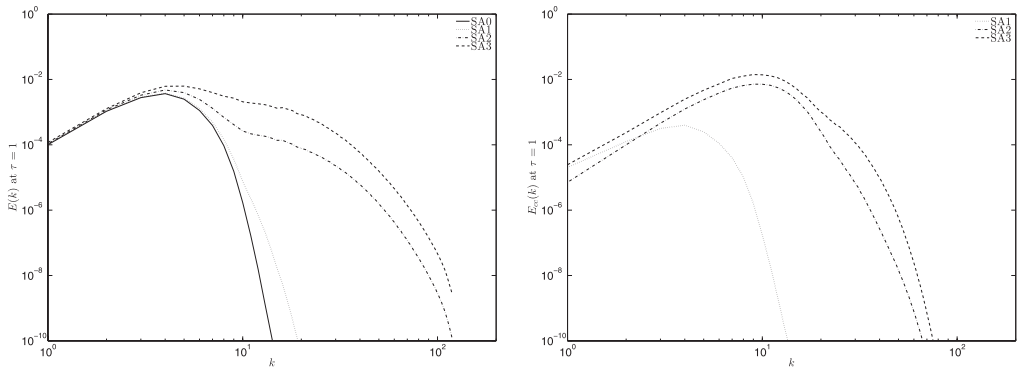

FIG. 4. Representation of the energy spectra (left column) and scalar spectra (right) as functions of the wavenumber for simulations SA presented in Table I, at time $\tau = 1$.

Variable viscosity effects tend to reduce the decay of kinetic energy as suggested by Figures 1 and 2. More precisely, the higher the initial variance of viscosity is, the smaller is the dissipation. This point is coherent with the phenomenology of higher Reynolds cases because the extra energy is due to smaller scales as shown by the spectra (see Figures 4 and 5). Note that the influence of variable viscosity does not last and the curves tend to collapse asymptotically at later time. In fact, the variance of the scalar c is also dissipated in the simulations due to the diffusion term proportional to κ. As a consequence, the variable viscosity term in the velocity equation is damped.

By contrast, simulations SA2 and SA3 have a higher Prandtl number ($\mathcal{P}_r = 50$), which enables viscosity fluctuations to persist longer. Although the mean Reynolds number is very low in these simulations ($Re = 0.17$), spectra shows that energy is spread on a broader range of wavenumbers than the constant viscosity case SA0 (see Figure 4). In addition to having high Prandtl number, SA3 has high initial variance of viscosity such that the flow have either $\nu_{\text{tot}} = \nu_{\text{min}}$ or $\nu_{\text{tot}} = \nu_{\text{max}}$. It is interesting to observe that zones of intense kinetic energy may survive in regions corresponding to low viscosity as shown by Figure 7. Therefore, turbulent eddies are confined and evolve in regions of low and almost uniform viscosity. The flow in low viscosity regions has a higher Reynolds number. In this context, the development of a spectra tail in Figure 4 can be interpreted as a regain of importance of transfer terms compared to viscous ones. Of course, one needs to be very cautious because this picture is only valid as long as exchanges of energy between high and low viscosity regions can be neglected. This preliminary analysis needs to be corroborated within a theoretical framework.

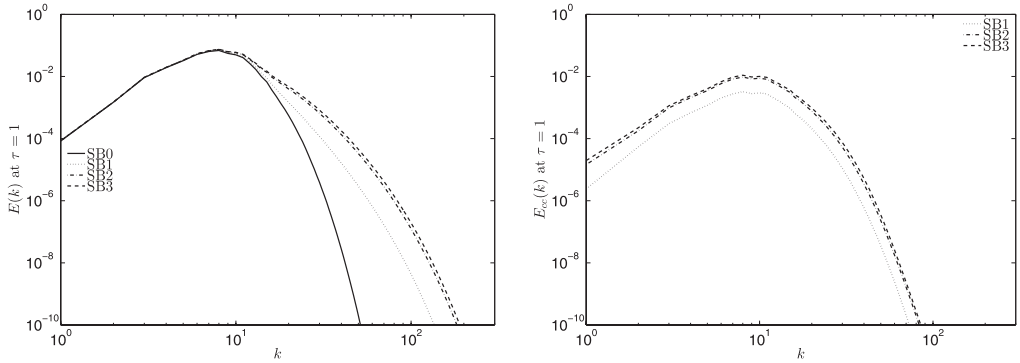

FIG. 5. Representation of the energy spectra (left column) and scalar spectra (right) as functions of the wavenumber for simulations SB presented in Table I, at time $\tau = 1$.

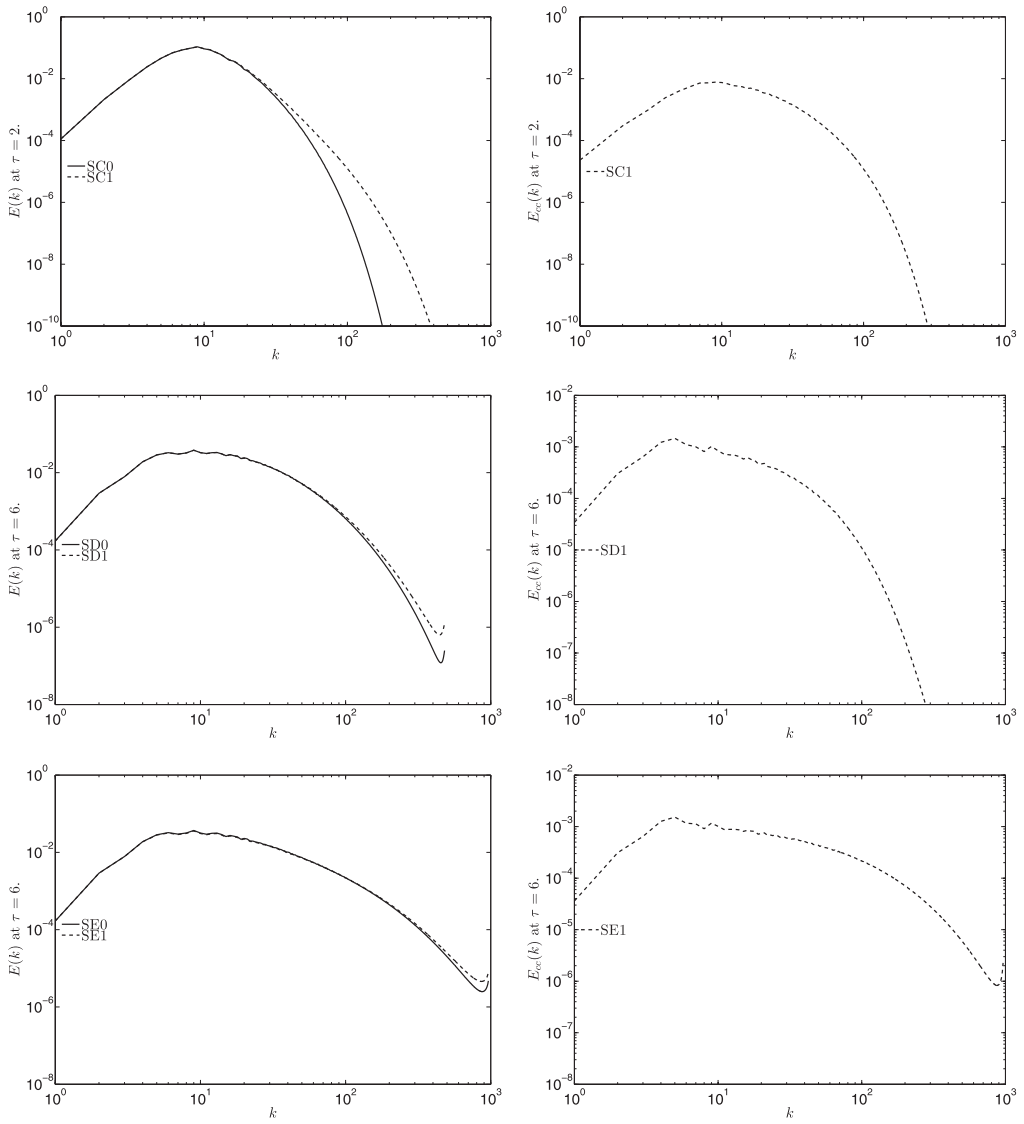

FIG. 6. Representation of the energy spectra (left column) and scalar spectra (right) as functions of the wavenumber for simulations SC (top), SD (middle), and SE (bottom) presented in Table I, at time $\tau = 2$ (top), $\tau = 6$ (middle) and $\tau = 6$ (bottom).

IV. STATISTICAL APPROACH

In order to interpret the effects of variable viscosity observed in the simulations and investigate the way it contributes to a diminution of the dissipation, we propose a statistical method. To this purpose, we build an EDQNM model. This type of closure has been indeed successfully used to model different types of turbulent flows such as isotropic turbulence,[19] the evolution of a passive scalar with[20,21] or without mean gradient,[15] stratification or rotation effects,[22,23] and premixed turbulent flame propagation.[24] Therefore, Sec. IV A is dedicated to the derivation of an EDQNM model while Sec. IV B gives comparisons to DNS. In Sec. IV C, the concept of an effective viscosity is proposed to evaluate variable viscosity effects.

A. Eddy-damped quasi-normal Markovian (EDQNM) approach

We write the equations of momentum Eq. (2a) in Fourier space. Fourier quantities as a function of the wave vector $\mathbf{k}$ are identified by $\hat{*}$. The reduced pressure can be eliminated by solving the

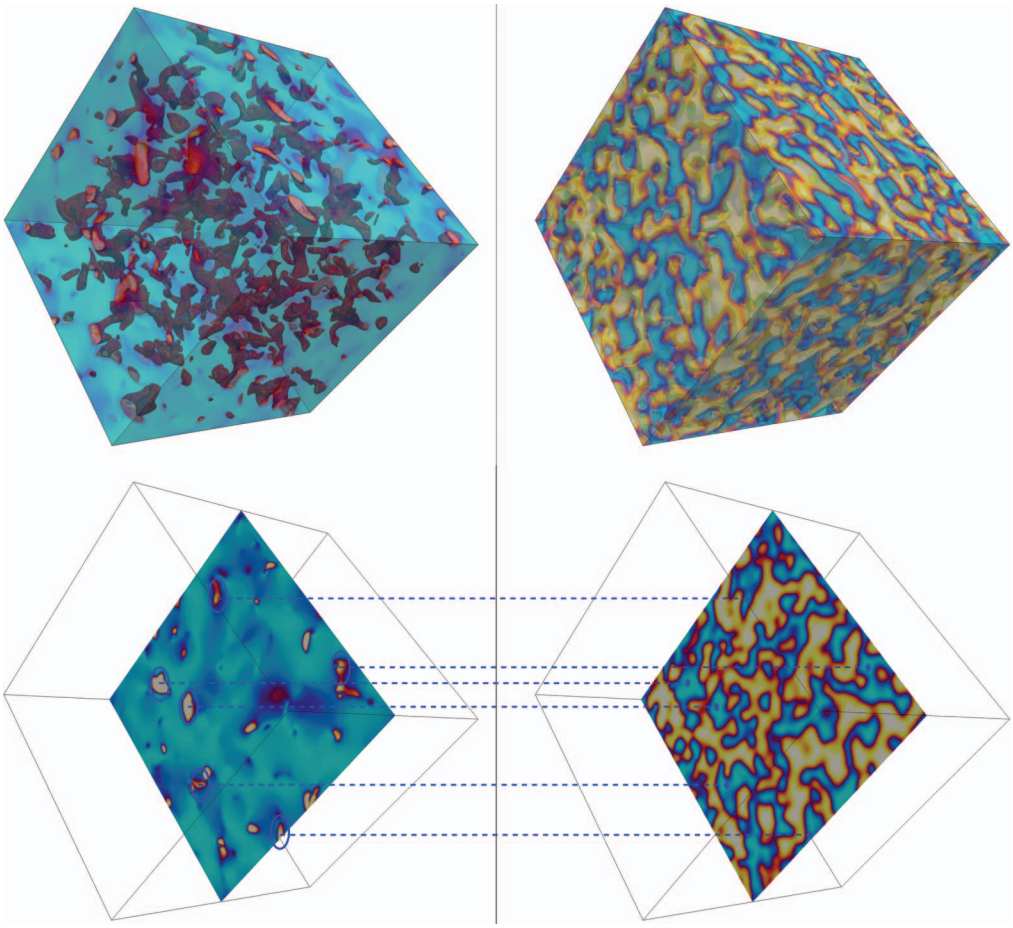

FIG. 7. Visualization at $\tau = 1.65$ of the simulation SA3. Left: 3D representation of kinetic energy (top) and cut at middle plane (bottom). High values of kinetic energy are represented in red while lower values are in blue. Right : Representation of the viscosity: low viscosity regions are in blue and high viscosity regions are in yellow. Blue dashed lines show the correspondence between turbulent structures and low viscosity regions.

Poisson equation such that we have:

$$\left(\partial_t + \nu k^2\right)\hat{u}_i(\mathbf{k},t) = -\frac{I}{2}P_{ijn}(\mathbf{k})\iiint \hat{u}_j(\mathbf{p})\hat{u}_n(\mathbf{k}-\mathbf{p})d\mathbf{p} \qquad (5)$$
$$-\mathcal{V}P_{in}(\mathbf{k})\iiint k_j p_j \hat{c}(\mathbf{k}-\mathbf{p},t)\hat{u}_n(\mathbf{p},t)d\mathbf{p},$$

with I the imaginary unit number, $P_{in}(\mathbf{k}) = \delta_{in} - k_i k_n/k^2$ the projector operator, δ_{in} the Kroenecker symbol, k the modulus of wave vector $\mathbf{k}$, and $P_{ijn}(\mathbf{k}) = k_j P_{in}(\mathbf{k}) + k_n P_{ij}(\mathbf{k})$ the Kraichnan operator. In Eq. (5), quadratic nonlinearities between the velocity and itself or the concentration give rise to a convolution product in Fourier space. The last term at the right-hand side accounts for variable viscosity, it also expresses through $P_{in}(\mathbf{k})$ the effects of redistribution by pressure. This is simply due to the fact that the variable viscosity term is not divergence free. The term proportional to the Kraichnan operator in Eq. (5) represents the classical nonlinear advection term and similarly its redistribution by pressure (see Ref. 25).

In an EDQNM approach, turbulence is described by the second order moments which are in our case, the spectrum $E(k)$ related to kinetic energy $E_T = \int_0^{+\infty} E(k)dk$ and the scalar spectrum $E_{cc}(k)$ with $\langle cc\rangle/2 = \int_0^{+\infty} E_{cc}(k)dk$. Now, we follow the method proposed by Orszag[25] in order to derive an EDQNM closure for the nonlinear variable viscosity term (see Appendix A). An important

assumption is isotropy as it implies that the cross spectra between velocity and the scalar c vanish. This leads to the following equation for the energy spectrum (or Lin equation):

$$\left(\partial_t + 2\nu k^2\right) E(k,t) = T(k,t) + \Pi(k,t), \tag{6}$$

with the transfer and variable viscosity term, respectively $T(k, t)$ and $\Pi(k, t)$, given by

$$T(k,t) = \iint_{\Delta_k} \Theta^T_{kpq} \frac{k}{pq} E(q,t) b(k,p,q) \left(k^2 E(p,t) - p^2 E(k,t)\right) dpdq, \tag{7a}$$

$$\Pi(k,t) = \mathcal{V}^2 \iint_{\Delta_k} \Theta^\Pi_{kpq} \frac{pk}{q} E_{cc}(q,t)(1+z^2)z^2 \left(k^2 E(p,t) + p^2 E(k,t)\right) dpdq. \tag{7b}$$

The transfer term $T(k, t)$ in Eq. (7a) is the well known expression in EDQNM for homogeneous isotropic turbulence originally proposed by Orszag.[19] The nonlinear viscous effects expressed by $\Pi(k, t)$ are detailed in Eq. (7b), this expression is the central result of this work. The integration domain on plane (p, q), Δ_k, is defined such that triads of wave vectors exist, $\mathbf{p} + \mathbf{q} + \mathbf{k} = 0$, (see Ref. 25). The geometric parameter b appearing in the classical EDQNM transfer term is given by $b(k, p, q) = p(xy + z^3)/k$. The coefficient z is the cosine of the angle between $\mathbf{k}$ and $\mathbf{p}$ in the triad, $z = (k^2 + p^2 - q^2)/2kp$. The coefficients x, y are defined similarly from the other inner angles of the triad. In addition, the characteristic times Θ^T_{kpq}, Θ^Π_{kpq} appearing during the combined Markovianization and eddy-damping process, are given by the following expressions:

$$\Theta^T_{kpq}(k,p,q,t) = \frac{1 - \exp\left(-\left[\nu(k^2+p^2+q^2) + \mu(k) + \mu(p) + \mu(q)\right]t\right)}{\nu(k^2+p^2+q^2) + \mu(k) + \mu(p) + \mu(q)}, \tag{8a}$$

$$\Theta^\Pi_{kpq}(k,p,q,t) = \frac{1 - \exp\left(-\left[\nu(k^2+p^2) + \mu'(k) + \mu'(p) + \kappa q^2 + \mu''(q)\right]t\right)}{\nu(k^2+p^2) + \mu'(k) + \mu'(p) + \kappa q^2 + \mu''(q)}, \tag{8b}$$

where μ, μ', and μ'' are relaxation rates for the different triple correlations. The specific terms μ' and μ'' due to variable viscosity need to be closed and are arbitrary chosen equal to the classical expression first proposed by Ref. 26, for μ, such that

$$\mu(k) = a_0 \left(\int_0^k p^2 E(p,t) dp\right)^{1/2}, \tag{9a}$$

$$\mu'(k) = a_1 \left(\int_0^k p^2 E(p,t) dp\right)^{1/2}, \tag{9b}$$

$$\mu''(k) = a_2 \left(\int_0^k p^2 E(p,t) dp\right)^{1/2}. \tag{9c}$$

In Eqs. (9a)–(9c), a_0, a_1, and a_2 are adjustable parameters. The value taken for a_0 is generally 0.36 in classical isotropic EDQNM models in order to recover the Kolmogorov constant value. In our case, for the sake of simplicity, we choose all the parameters equal, $a_0 = a_1 = a_2 = 0.36$.

In order to get a complete model, it is also necessary to add an equation for the scalar spectrum. Its complete expression is classical and can be found for instance in Lesieur.[15] It is straightforward to see that variable viscosity terms do not modify this equation in the isotropic case. Again, we take the classical value 0.36 for the different constants.

Now, we derive the equation for kinetic energy by integrating Eq. (7b) with respect to k:

$$\frac{dE_T}{dt} = -\left(\underbrace{2\nu \int_0^{+\infty} k^2 E(k,t) dk}_{\varepsilon_a} \underbrace{- \mathcal{V}^2 \int_0^{+\infty} dk \iint_{\Delta_k} \Theta^\Pi_{kpq} \frac{pk}{q} E_{cc}(q,t)(1+z^2)z^2 \left(k^2 E(p,t) + p^2 E(k,t)\right) dpdq}_{\varepsilon_b} \right). \tag{10}$$

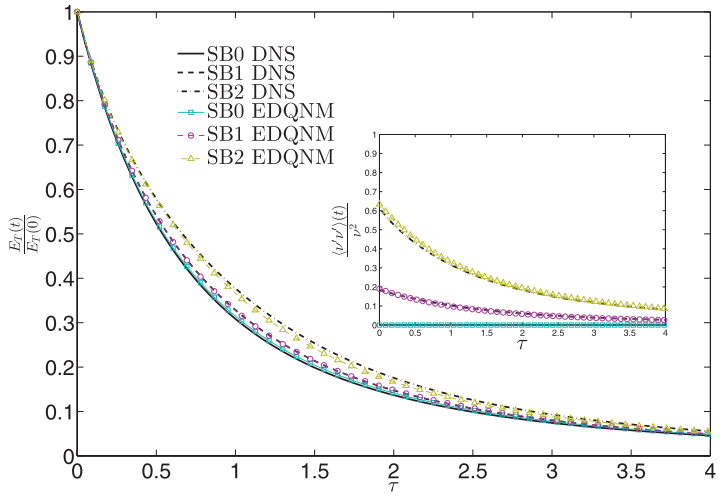

FIG. 8. Evolution of turbulent kinetic energy as a function of time for the simulations SB-0,1,2 compared to EDQNM model. Inset: Evolution of the variance of viscosity fluctuations as a function of time.

The term ε_a and ε_b have been already defined in Eq. (3). Remark also that the integral of $T(k, t)$ over wave numbers vanishes by definition of the transfer. We immediately note that ε_b is negative in the EDQNM closure. This clearly shows that variable viscosity effects contribute to reducing the dissipation of kinetic energy, as observed in the simulations.

B. Comparison DNS/EDQNM

In this section, we present different comparisons between DNS and the EDQNM isotropic model, in order to validate the closure for the variable viscosity term and to assess the merits of our statistical approach.

To begin with, we give some details about our EDQNM code. The numerical integration of Eq. (6) follows the standard procedure proposed by Ref. 27. We use a logarithmic discretization for the wavenumbers, such that $k_n = k_0 2^{n/F}$. The most difficult and time-consuming part of the procedure concerns the evaluation of the different integrals $\iint_{\Delta_k} dpdq$. We use the same scheme as in Ref. 27 which preserves symmetries and integral properties of the continuous equations as for instance $\int_0^{+\infty} T(k)dk = 0$.

We have tested the convergence up to $F = 30$ which allows to minimize numerical errors due to elongated triads. In particular, the ratio between smallest and largest sides of triad should verify $\frac{\min[k,p,q]}{\max[k,p,q]} \geq 2^{1/F} - 1$ as proposed by Ref. 15. This criterion is satisfied in the cases presented here for triads having a side in the energetic wavenumbers and another one where viscosity effects are significant at larger wavenumbers. As we will see, distant interactions are important in this problem and to account for their effects, the code needs analytical corrections similar to those in Lesieur and Schertzer[28] for high Reynolds number configurations.

Also, caution must be taken when comparing DNS and EDQNM as the former simulates a particular realization while the latter models statistical quantities. In addition, there is a bias because the different fields are uncorrelated at the beginning of the DNS leading to initially null triple correlations. On the contrary in EDQNM, triple correlations are modelled and have non-zero values from start.

When looking at the time evolutions of kinetic energy, the EDQNM predictions are in relatively good agreement with the DNS as shown by Figure 8. At later times, a slight underestimation of viscosity effects is observed in all our comparisons. This tendency is more visible on cases where the initial variance of viscosity is high.

We propose the comparison between DNS and EDQNM on spectra in Figure 9. EDQNM seems to correctly predict the evolution of low and energetic wavenumbers. The trend to have

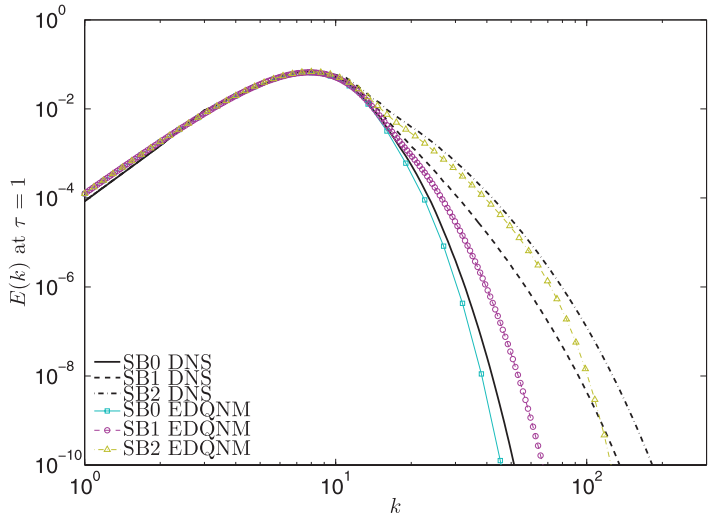

FIG. 9. Representation of energy spectra at time $\tau = 1$ for simulations and EDQNM SB-0,1,2.

additional energy at larger wavenumbers characterizing variable viscosity effects is qualitatively well reproduced in EDQNM. We clearly observe a discrepancy, specially at large wavenumbers. This may explain the underestimation of variable viscosity effects in EDQNM compared to DNS. The origin of this flaw may probably come from the form of the eddy damping terms μ', μ'' expressing the closure of the fourth order cumulants. In fact, their expressions are not well justified here as they are directly inspired from the closure for μ appearing in the transfer $T(k, t)$. Note that the tendency to underestimate energy of small scales is also observed in constant viscosity EDQNM. This point, still discussed in the turbulence community, is sometimes attributed to the fact that intermittency effects are not taken into account in the model (see Ref. 15).

Despite some defects already mentioned, the EDQNM approach successfully reproduce the diminution of dissipation in variable viscosity turbulence and also the persistence of energy in the small scales. As a consequence, EDQNM is an interesting theoretical framework to interpret DNS results and to analyse in depth the effects of the variable viscosity term.

C. The effective viscosity ν_{eff}

In this part, we try to interpret further the expression for the variable viscosity term, $\Pi(k, t)$, in Eq. (7b). The objective is to derive a simple relation accounting for variable viscosity effects. Then, we will test the validity of the formula in the simulations.

In order to proceed, we need first to have an idea of which wavenumbers k have important contributions to variable viscosity effects. In particular, the relative position of energy and scalar spectra compared to these particular k has to be specified. At large Reynolds numbers, as suggested by the simulations, $\Pi(k, t)$ is expected to be negligible compared to $T(k, t)$ in the inertial range and at low wavenumbers. The main influence of $\Pi(k, t)$ is therefore expected to appear close to the peak of dissipation (maximum of $k^2E(k, t)$) which is well separated from the maxima of the energy spectrum and more importantly the scalar spectrum. In this case, we propose an approximation for Eq. (7b) based on distant interactions between wavenumbers k, p, q appearing in the triadic integral. Its complete derivation is fully detailed in Appendix B and corresponds to the case (I) with $q \ll p \sim k$. This approximation assumes also large t in order to simplify the characteristic time Θ^{Π}_{kpq}. It gives

$$\Pi(k, t) \sim 2\frac{\langle \nu' \nu' \rangle}{\nu} k^2 E(k, t). \tag{11}$$

Substituting Eq. (11) in Eq. (6) demonstrates that at leading order and around the dissipation maximum, the variable viscosity term behaves like a negative viscosity. Therefore, it is convenient

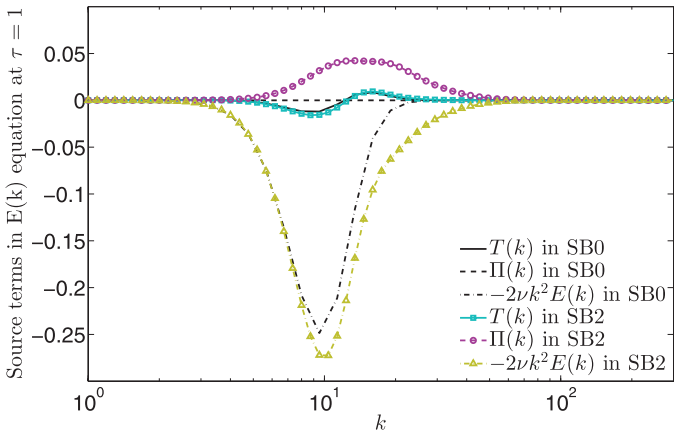

FIG. 10. Representation of the different transfer terms (advection, variable viscosity, and dissipation) in the equation for energy spectrum $E(k)$ at $\tau = 1$ for cases SB0 and SB2 from EDQNM simulations.

to introduce an effective viscosity derived from this EDQNM distant interactions approximation, noted $\nu_{\text{eff}}^{(I)}$:

$$\nu_{\text{eff}}^{(I)} = \nu \left(1 - \frac{\langle \nu' \nu' \rangle}{\nu^2}\right). \tag{12}$$

Equation (12) is a local expression accounting for the mean viscosity and its fluctuations. It is expected to be valid at wavenumbers k where dissipative effects are most active. Therefore, after integration over k, this formula should give a good global evaluation of all the viscous processes acting in the flow.

Now, we check this approximation with our EDQNM simulations. It can be examined for instance by looking at the different terms in the Lin equation, Eq. (6), respectively $-2\nu k^2 E(k, t)$, $T(k, t)$, and $\Pi(k, t)$. Their contributions are shown in Figure 10 for SB cases. The SB cases have very low Reynolds numbers so that transfer terms are very small compared to $2\nu k^2 E(k)$. However, when mean viscosity effects are strong, the variable viscosity term, $\Pi(k, t)$, is also important and tends to reduce the dissipation. As a result, small scales are less attenuated than expected, and this explains the presence of extra energy in the simulations. We see from Figure 10 that the maximum of $\Pi(k, t)$ is in fact located close to the maximum of dissipation although both maxima do not totally coincide here. We can verify the validity of the distant interactions approximation, Eq. (11), where the dissipation is important. For instance at $k = 15$, the ratio $\Pi(k, t)/2\nu k^2 E(k, t)$ with $\tau = 1$ in SB2 equals 0.32 which is close to the value of $\langle \nu' \nu' \rangle / \nu^2$ predicted by the distant interactions approximation.

The validity of approximation Eq. (12) can also be checked globally on the total dissipation after integration over wavenumbers. In fact, Eq. (12) embodies the idea that a flow with a variable viscosity coefficient behaves like a flow with a constant but smaller viscosity. In the simulations, the effective viscosity noted ν_{eff} can be directly measured from:

$$\frac{\nu_{\text{eff}}}{\nu} = \frac{-\frac{dE_T}{dt}}{\nu \langle \partial_i u_j \partial_i u_j \rangle} = \frac{\varepsilon_a + \varepsilon_b}{\varepsilon_a}, \tag{13}$$

where ε_a and ε_b are the terms composing the dissipation introduced in Eq. (3).

It is interesting to discuss the value of ν_{eff} as a function of the variance of viscosity. In Figure 11, we show the time evolution in plane $(\langle \nu' \nu' \rangle / \nu^2, \nu_{\text{eff}}/\nu)$ of all the DNS and the EDQNM simulation SB2. We also represent the approximation $\nu_{\text{eff}}^{(I)}$ derived from the EDQNM closure. First of all, we would like to report that the EDQNM simulation converge well to the approximation characterized by $\nu_{\text{eff}}^{(I)}$ as expected (although SB2 has a low Reynolds number). In the DNS, the trajectories start from $\nu_{\text{eff}} = \nu$ at $t = 0$ because, as already mentioned, the scalar and the velocity field are initially decorrelated such that the term ε_b in Eq. (3) equals zero. Rapidly, ν_{eff} decreases

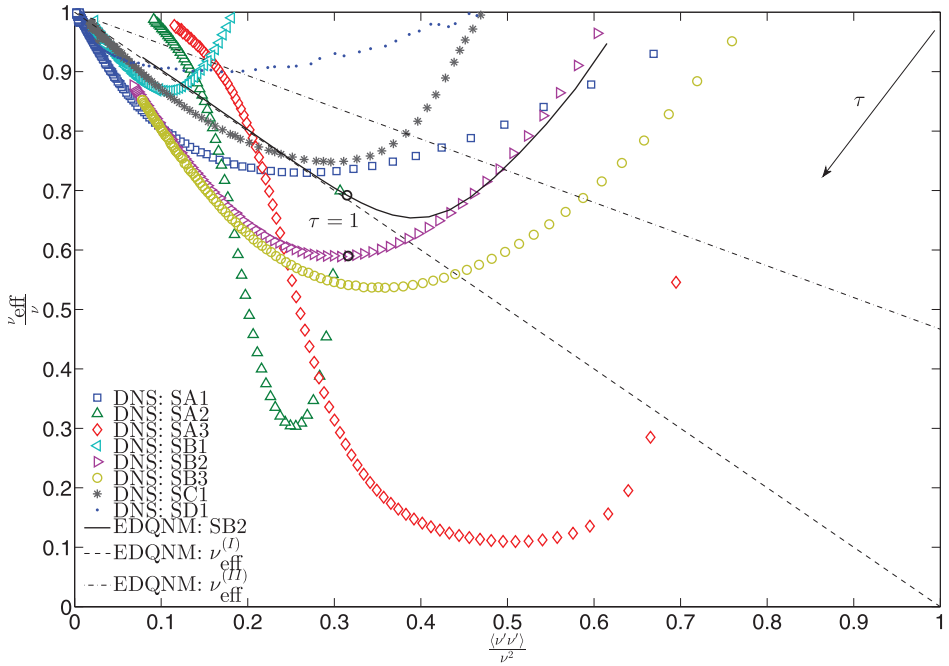

FIG. 11. Representation of the renormalized effective viscosity as a function of the renormalized variance of viscosity fluctuations. Lines: EDQNM simulation of SB2 and non-local expansion of the EDQNM closure $\nu_{\text{eff}}^{(I)}$ and $\nu_{\text{eff}}^{(II)}$. Symbols: Different simulations presented in Table I. Black circles: DNS and EDQNM simulations of SB2 at $\tau = 1$ corresponding to Figs. 9 and 10.

as a result of the appearance of variable viscosity effects. We can observe in some simulations that ε_b may have same order of magnitude as the dissipation ε_a. Afterwards, ν_{eff} grows while the fluctuations of viscosity tends to zero. During this second stage, the approximation deduced from EDQNM, $\nu_{\text{eff}}^{(I)}$, gives a higher value for ν_{eff}. This is not surprising as we have observed from comparisons with DNS, Figure 8, that the model underestimates variable viscosity effects. In Figure 11, we also indicate the position at $\tau = 1$ of EDQNM and DNS SB2 simulation corresponding to spectra in Figure 9 and sources terms of Lin equation in Figure 10. We see that the effective viscosities ν_{eff} from DNS and EDQNM already differ although, looking at the comparisons between kinetic energy evolution (Figure 8), the different DNS/EDQNM curves are close. In fact, the representation in plane $(\langle\nu'\nu'\rangle/\nu^2, \nu_{\text{eff}}/\nu)$ magnifies the distances between EDQNM and DNS.

The two simulations SA2 and SA3, corresponding to high Prandtl number, seem to behave differently. During the first stage, variable viscosity effects become much stronger compared to the other cases. In fact, the variance of viscosity can maintain itself longer and variable viscosity effects have more time to develop. Also, as observed in Figure 7, turbulent kinetic energy accumulates in low viscosity regions. There, the low viscosity value ν_{min}, much smaller than the mean value ν, may give a first approximation for the effective viscosity of the flow ($\nu_{\text{min}}/\nu = 0.02$ in SA2-3). During the second stage, when variable viscosity effects tend to diminish, the effective viscosity is much smaller than expected. In particular, the distant interactions approximation of EDQNM, $\nu_{\text{eff}}^{(I)}$, seems to overpredict variable viscosity effects (while it underestimates it in the other cases). We propose the following argument to explain this phenomenon. First, we note that the maximum of the scalar spectra, initially at $k_{peak} = 10$, do not evolve much in the high Prandtl number simulations. By contrast, the maximum of energy spectra is shifted toward the small wavenumbers as shown in Figure 4. In fact, the Reynolds number is very low such that at first order $E(k, t) = E(k, 0)\exp[-2\nu k^2 t]$ and $E_{cc}(k, t) = E_{cc}(k, 0)\exp[-2\kappa k^2 t]$. Therefore, the maxima of $E(k, t)$ and $E_{cc}(k, t)$ separate when $\kappa \ll \nu$. Then in Appendix B, we derive a second type of distant interactions approximation corresponding to case (II), $k \ll p \sim q$, which seems better suited for these cases. This gives from

Eq. (B6) and assuming $\kappa \ll \nu$:

$$\nu_{\text{eff}}^{(II)} = \nu \left(1 - \frac{8}{15} \frac{\langle \nu' \nu' \rangle}{\nu^2}\right). \tag{14}$$

In Figure 11, we see in fact that the approximation $\nu_{\text{eff}}^{(II)}$ from Eq. (14) is closer to the final stage of SA2 and SA3. But in addition, we would like to remind that the distribution of viscosity is nearly bi-modal in these simulations due to the relatively high Prandtl number ($\mathcal{P}_r = 50$) and strong initial variance $\langle \nu' \nu' \rangle$. As a consequence, the distribution of c is far from Gaussianity. As already mentioned, in the EDQNM model, fourth order cumulants expressing this deviation from Gaussianity are modelled by the eddy damping term. This is the weak point of our model and it probably explains the origin of the discrepancy between DNS/EDQNM.

Finally, we would like to mention that a simple approximation as Eq. (12) can be of practical interest for modelling flows with strong variations of viscosity. Since the variance of viscosity can be directly expressed using the second order scalar correlation, which is usually computed in turbulence models, Eq. (12) can be utilized to modify terms depending on physical viscosity.

V. CONCLUSION

In this study, we have investigated by the means of DNS the decay of homogeneous isotropic turbulence in a variable viscosity fluid. Variable viscosity effects have been found negligible on the overall turbulent kinetic energy at high Reynolds numbers as proposed by Taylor's postulate. However, we have observed significant differences with constant viscosity cases at moderate and low Reynolds numbers. In these configurations, turbulence can maintain itself longer, particularly if the variance of viscosity is important. More precisely, while in the high viscosity regions the flow becomes laminar, the initial turbulent kinetic energy survives and can be transferred to the small scales in low viscosity regions as shown by spectra. We may call "lumpy" turbulence this coexistence of a laminar and a turbulent phase at the same time, entangled in low and high viscosity regions.

In order to explain this physics, we propose the theory that a variable viscosity fluid behaves like a fluid with constant but lower average viscosity coefficient. We justify this idea by developing an EDQNM spectral closure for the additional variable viscosity term. The resulting model has been able to successfully reproduce the variable viscosity effects despite a slight underestimation of their intensity as shown by the comparisons with DNS. It clearly establishes that variable viscosity effects diminish the value of dissipation as observed. In addition, the role of distant interactions between the characteristic length of the viscosity fluctuations and the length of small turbulent eddies have been identified through an asymptotic expansion of our EDQNM variable viscosity closure. Therefore, we are able to quantify the effective dissipation of the flow due to variable viscosity. At leading order, these effects can be perceived as an effective viscosity $\nu_{\text{eff}} = \nu \left(1 - \frac{\langle \nu' \nu' \rangle}{\nu^2}\right)$. We think this opens the path to possible simple corrections in one point-statistical turbulent models.

ACKNOWLEDGMENTS

We wish to acknowledge O. Soulard, P. Arnault, and A. Llor for many interesting discussions and support.

APPENDIX A: DERIVATION OF THE EDQNM CLOSURE

In order to get the EDQNM closure for the variable viscosity term, we follow the derivation proposed by Orszag.[25] Note that other methods exist, as for instance expansions used for the DIA model[29] which can be more efficient but also more complex.

First, we give the definitions for the different moments appearing in the statistical equations, using the 3D Dirac function δ:

$$S_{ij}(\mathbf{k})\delta(\mathbf{k}+\mathbf{p}) = \langle \hat{u}_i(\mathbf{k})\hat{u}_j(\mathbf{p})\rangle, \tag{A1a}$$

$$Q(\mathbf{k})\delta(\mathbf{k}+\mathbf{p}) = \langle \hat{c}(\mathbf{k})\hat{c}(\mathbf{p})\rangle, \tag{A1b}$$

$$K_{ij}(\mathbf{k},\mathbf{p})\delta(\mathbf{k}+\mathbf{p}+\mathbf{q}) = \langle \hat{u}_i(\mathbf{k})\hat{u}_j(\mathbf{p})\hat{c}(\mathbf{q})\rangle. \tag{A1c}$$

In this problem and as already mentioned, isotropy implies that the cross correlation between the scalar and the different components of velocity is zero $\langle \hat{u}_i(\mathbf{k})\hat{c}(\mathbf{p})\rangle = 0$. This leads to numerous simplifications when deriving the quasi-normal approximation. In particular, we have

$$\langle \hat{u}_i(\mathbf{k})\hat{u}_j(\mathbf{p})\hat{c}(\mathbf{q})\hat{c}(\mathbf{r})\rangle = S_{ij}(\mathbf{k})\delta(\mathbf{k}+\mathbf{p})Q(\mathbf{q})\delta(\mathbf{q}+\mathbf{r}), \tag{A2a}$$

$$\langle \hat{u}_i(\mathbf{k})\hat{u}_j(\mathbf{p})\hat{u}_l(\mathbf{q})\hat{c}(\mathbf{r})\rangle = 0. \tag{A2b}$$

The equation for the second moment is deduced from Eq. (5):

$$\begin{aligned}\left(\partial_t + 2\nu k^2\right) S_{ij}(\mathbf{k},t) = &-\mathcal{V}P_{in}(\mathbf{k})\iiint k_l p_l K_{jn}(-\mathbf{k},\mathbf{p},t)d\mathbf{p} \\ &+\mathcal{V}P_{jn}(\mathbf{k})\iiint k_l p_l K_{in}(\mathbf{k},\mathbf{p},t)d\mathbf{p} + T_{ij}(\mathbf{k},t).\end{aligned} \tag{A3}$$

Here, the nonlinear term coming from the advection and its redistribution by pressure is noted $T_{ij}(\mathbf{k},t)$.

We transform Eq. (A3) in order to obtain a more convenient expression using $K^*_{jn}(\mathbf{k},-\mathbf{p}) = K_{jn}(-\mathbf{k},\mathbf{p})$ (coming from the reality of u_i and c in physical space, $\hat{u}_i(\mathbf{k}) = \hat{u}_i^*(-\mathbf{k})$, $\hat{c}(\mathbf{k}) = \hat{c}^*(-\mathbf{k})$):

$$\begin{aligned}\left(\partial_t + 2\nu k^2\right) S_{ij}(\mathbf{k},t) = &-\mathcal{V}P_{in}(\mathbf{k})\iiint k_l p_l K^*_{jn}(\mathbf{k},-\mathbf{p},t)d\mathbf{p} \\ &+\mathcal{V}P_{jn}(\mathbf{k})\iiint k_l p_l K_{in}(\mathbf{k},\mathbf{p},t)d\mathbf{p} + T_{ij}(\mathbf{k},t).\end{aligned} \tag{A4}$$

It leads by a change of variable $\mathbf{p} \to -\mathbf{p}$ in the first integral to

$$\begin{aligned}\left(\partial_t + 2\nu k^2\right) S_{ij}(\mathbf{k},t) = &+\mathcal{V}P_{in}(\mathbf{k})\iiint k_l p_l K^*_{jn}(\mathbf{k},\mathbf{p},t)d\mathbf{p} \\ &+\mathcal{V}P_{jn}(\mathbf{k})\iiint k_l p_l K_{in}(\mathbf{k},\mathbf{p},t)d\mathbf{p} + T_{ij}(\mathbf{k},t).\end{aligned} \tag{A5}$$

Similarly, we write the equation for the third moment

$$\begin{aligned}\left(\partial_t + \nu k^2 + \nu p^2 + \frac{\nu}{\mathcal{P}_r}|\mathbf{k}+\mathbf{p}|^2\right) K_{ij}(\mathbf{k},\mathbf{p},t) = &+\mathcal{V}P_{in}(\mathbf{k})k_l p_l S_{jn}(\mathbf{p},t)Q(\mathbf{q},t) \\ &+\mathcal{V}P_{jn}(\mathbf{p})k_l p_l S_{in}(\mathbf{k},t)Q(\mathbf{q},t),\end{aligned} \tag{A6}$$

where in Eq. (A6), $\mathbf{q} = -\mathbf{k} - \mathbf{p}$. Time-integrating the previous equation yields:

$$\begin{aligned}K_{ij}(\mathbf{k},\mathbf{p},t) = \mathcal{V}\int_0^t ds\, &\exp\left[-\nu(k^2+p^2+q^2/\mathcal{P}_r)(t-s)\right]\times \\ &\left(P_{in}(\mathbf{k})S_{jn}(\mathbf{p},s) + P_{jn}(\mathbf{p})S_{in}(\mathbf{k},s)\right) p_l k_l Q(\mathbf{q},s).\end{aligned} \tag{A7}$$

In order to derive the EDQNM closure, we reinject this integro-differential equation, Eq. (A7), into the equation for the second order correlation Eq. (A5). We remark that for isotropic turbulence

$S^*_{ij}(\mathbf{k}) = S_{ij}(\mathbf{k})$, and we have always $Q^*(\mathbf{k}) = Q(\mathbf{k})$.

$$\begin{aligned}\left(\partial_t + 2\nu k^2\right) S_{ij}(\mathbf{k},t) = \mathcal{V}^2 \iiint d\mathbf{p} \int_0^t ds \exp\left[-\nu(k^2+p^2+q^2/\mathcal{P}_r)(t-s)\right] \times \\ P_{im}(\mathbf{k})(k_l p_l)^2 \left(P_{jn}(\mathbf{k})S_{mn}(\mathbf{p},s) + P_{mn}(\mathbf{p})S_{jn}(\mathbf{k},s)\right) Q(\mathbf{q},s) \\ + \mathcal{V}^2 \iiint d\mathbf{p} \int_0^t ds \exp\left[-\nu(k^2+p^2+q^2/\mathcal{P}_r)(t-s)\right] \times \\ P_{jm}(\mathbf{k})(k_l p_l)^2 \left(P_{in}(\mathbf{k})S_{mn}(\mathbf{p},s) + P_{mn}(\mathbf{p})S_{in}(\mathbf{k},s)\right) Q(\mathbf{q},s) + T_{ij}(\mathbf{k},t). \end{aligned} \tag{A8}$$

In order to obtain the equation for energy, it is sufficient to consider the trace only

$$\begin{aligned}\left(\partial_t + 2\nu k^2\right) S_{ii}(\mathbf{k},t) = 2\mathcal{V}^2 \iiint d\mathbf{p} \int_0^t ds \exp\left[-\nu(k^2+p^2+q^2/\mathcal{P}_r)(t-s)\right] \times \\ P_{im}(\mathbf{k})(k_j p_j)^2 \left(P_{in}(\mathbf{k})S_{mn}(\mathbf{p},s) + P_{mn}(\mathbf{p})S_{in}(\mathbf{k},s)\right) Q(\mathbf{q},s) + T_{ii}(\mathbf{k},t). \end{aligned} \tag{A9}$$

Now, the isotropic second order correlation tensor for velocity takes the form $S_{ij}(\mathbf{k}) = \frac{E(k)}{4\pi k^2} P_{ij}(\mathbf{k})$. Concerning the scalar density, isotropy simply implies $Q(\mathbf{k}) = \frac{E_{cc}(k)}{2\pi k^2}$. The equation is also Markovianized, introducing the classical characteristic time Θ_{kpq}:

$$\begin{aligned}\left(\partial_t + 2\nu k^2\right) S_{ii}(\mathbf{k},t) = 2\mathcal{V}^2 \iiint d\mathbf{p}\Theta_{kpq} Q(\mathbf{q},t) P_{im}(\mathbf{k})(k_j p_j)^2 \left(P_{in}(\mathbf{k})S_{mn}(\mathbf{p},t) + P_{mn}(\mathbf{p})S_{in}(\mathbf{k},t)\right) \\ + T_{ii}(\mathbf{k},t). \end{aligned} \tag{A10}$$

Substituting for S_{ii} and Q, E and E_{cc} gives:

$$\begin{aligned}\left(\partial_t + 2\nu k^2\right) \frac{E(k,t)}{4\pi k^2} = \mathcal{V}^2 \iiint d\mathbf{p}\Theta_{kpq} \frac{E_{cc}(q,t)}{2\pi q^2} (k_j p_j)^2 P_{mn}(\mathbf{k}) P_{mn}(\mathbf{p}) \left(\frac{E(p,t)}{4\pi p^2} + \frac{E(k,t)}{4\pi k^2}\right) \\ + \frac{T(k,t)}{4\pi k^2}. \end{aligned} \tag{A11}$$

We use the following simplifications (see Ref. 19) with z the cosine of the angle between $\mathbf{k}$ and $\mathbf{p}$:

$$(k_j p_j)^2 = p^2 k^2 z^2, \tag{A12}$$

$$P_{mn}(\mathbf{k}) P_{mn}(\mathbf{p}) = 1 + z^2, \tag{A13}$$

such that we have:

$$\begin{aligned}\left(\partial_t + 2\nu k^2\right) \frac{E(k,t)}{4\pi k^2} = \mathcal{V}^2 \iiint d\mathbf{p}\Theta_{kpq} \frac{E_{cc}(q,t)}{2\pi q^2} (1+z^2) p^2 k^2 z^2 \left(\frac{E(p,t)}{4\pi p^2} + \frac{E(k,t)}{4\pi k^2}\right) \\ + \frac{T(k,t)}{4\pi k^2}. \end{aligned} \tag{A14}$$

We use the change of variable:

$$\iiint F(k,p,q) d\mathbf{p} = 2\pi \iint_{\Delta_k} \frac{pq}{k} F(k,p,q) dpdq. \tag{A15}$$

So that we obtain the final equation, Eq. (7b).

APPENDIX B: DERIVATION OF THE DISTANT INTERACTION APPROXIMATIONS

In this section, we propose to derive an approximation of the EDQNM closure for the variable viscosity term $\Pi(k,t)$, Eq. (7b). In order to proceed, we need to evaluate the triadic integral $\iint_{\Delta_k} dpdq$.

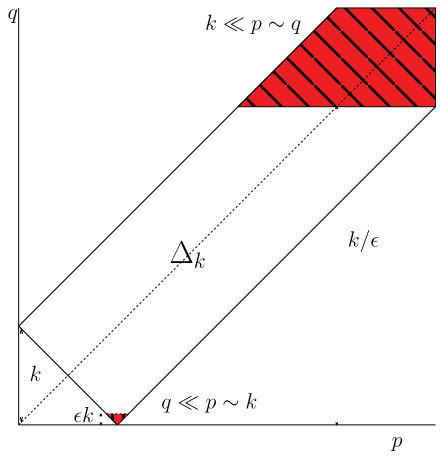

FIG. 12. Representation in the plane (p, q) of the domain of integration Δ_k for the EDQNM closure. The coloured zones represents the two different types of distant interactions leading to the expression for the effective viscosity.

Figure 12 represents the integration domain for a given wave number k. Here, we show the existence of specific cases where it is possible to simplify the integral.

Case (*I*): $q \ll p \sim k$

First, let us assume that the peak of the scalar spectra is located at very small wave numbers compared to the peak of energy spectra as in Figure 13 (left). If we are interested in looking at wavenumbers k where kinetic energy is important, then the integrated term in Eq. (7b) is significant when q is small compared to the wavenumber k. From Figure 12, we immediately see that the main contribution of the triadic integral comes from the small corner $q \ll p \sim k$. It is important to stress that this configuration does not only occur when $E_{cc}(k, t)$ and $E(k, t)$ are well separated. For instance, it is important to look at contributions of variable viscosity effects at the peak of $k^2E(k, t)$ corresponding to maximum of dissipation. This peak is usually at larger wavenumbers and well separated from the maxima of $E(k, t)$ and $E_{cc}(k, t)$. Therefore, the contribution in the triadic integral is also expected in this case to come from q close the maximum of E_{cc} and p near k at maximum of $k^2E(k, t)$.

In this context, we derive the distant approximation of Eq. (7b). Introducing a small parameter ϵ such that $q/k \leq \epsilon$ and $\int_0^{+\infty} E_{cc}(q, t)dq \sim \int_0^{\epsilon k} E_{cc}(q, t)dq$, we can write

$$\Pi(k, t) = \mathcal{V}^2 \iint_{\Delta_k} \Theta^{\Pi}_{kpq} \frac{pk}{q} E_{cc}(q, t)(1 + z^2)z^2 \left(k^2E(p, t) + p^2E(k, t)\right) dpdq, \tag{B1a}$$

$$\approx \mathcal{V}^2 \int_0^{\epsilon k} \left(\int_{k-q}^{k+q} \Theta^{\Pi}_{kpq} \frac{pk}{q} E_{cc}(q, t)(1 + z^2)z^2 \left(k^2E(p, t) + p^2E(k, t)\right) dp \right) dq. \tag{B1b}$$

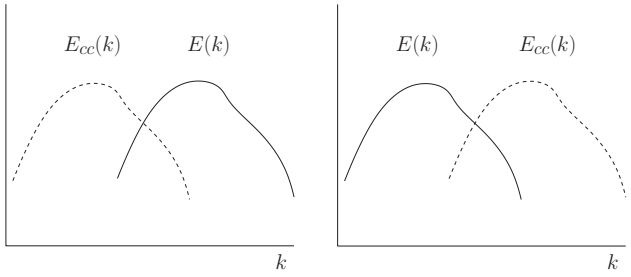

FIG. 13. Representation of the assumptions on the relative position of energy and scalar spectra leading to the derivation of the two distant interaction approximations expressing the variable viscosity effects. Left: case (I) $q \ll p \sim k$, Right: case (II) $k \ll p \sim q$.

Then, we evaluate the integral over p in Eq. (B1b) using Taylor expansion around k of terms depending of p. In particular, we have at first order $E(p,t) \sim E(k,t)$, $z \sim 1$, $\Theta^{\Pi}_{kpq} \sim \Theta^{\Pi}_{kkq}$. This leads to

$$\Pi(k,t) \approx \mathcal{V}^2 8k^4 E(k,t)\Theta^{\Pi}_{kk0} \int_0^{\epsilon k} E_{cc}(q,t)dq, \tag{B2a}$$

$$\approx \mathcal{V}^2 4k^4 E(k,t)\Theta^{\Pi}_{kk0}\langle cc\rangle, \tag{B2b}$$

$$\approx 4\langle \nu'\nu'\rangle k^4 \Theta^{\Pi}_{kk0}(k,t)E(k,t). \tag{B2c}$$

At this stage, Eq. (B2c) gives a distant approximation depending on the characteristic time $\Theta^{\Pi}_{kk0}(k,t)$. To simplify this expression further, we assume:

1. $t \to +\infty$
2. k is large enough such that $\mu'(k) \ll \nu k^2$.

The second assumption is strong and can be justified as follows: at large k, $E(k,t)$ usually decreases such that $\mu(k)$ is not growing like k^2. Note that *a priori* these additional hypotheses are not directly related to the distance between wave numbers q and k. Using the definition for the Markovian time Θ^{Π} Eq. (8b), we obtain:

$$\Theta^{\Pi}_{kk0}(k, t \to +\infty) \approx 1/2\nu k^2. \tag{B3}$$

Injecting this expression into Eq. (B2c) leads to

$$\Pi(k,t) \approx 2\frac{\langle \nu'\nu'\rangle}{\nu} k^2 E(k,t). \tag{B4}$$

In this expression, Eq. (B4), the variable viscosity contributions are proportional to $k^2E(k,t)$ which suggests that they behave as a negative viscosity term.

Case (II): $k \ll p \sim q$

There is another situation where it is possible to derive a distant approximation for the variable viscosity term. We assume that the energy spectrum has a maximum at smaller wave numbers than the scalar spectrum as suggested by Figure 13 (right). This means that the characteristic length of the turbulent eddies is much larger than characteristic length of viscosity variations. In this case, the interesting wavenumber k for the energy spectra to look at will be much smaller than q. Therefore, the main contribution in the triadic integral for the variable viscosity terms will come from the $k \ll p \sim q$ corner as represented in Figure 12. We introduce again a small parameter ϵ such that $k \leq \epsilon q$ and $\int_0^{+\infty} E_{cc}(q,t)dq \sim \int_{k/\epsilon}^{+\infty} E_{cc}(q,t)dq$. We have

$$\Pi(k,t) \approx \mathcal{V}^2 \int_{k/\epsilon}^{+\infty} \left(\int_{q-k}^{q+k} \Theta^{\Pi}_{kpq} \frac{pk}{q} E_{cc}(q,t)(1+z^2)z^2 \left(k^2E(p,t) + p^2E(k,t)\right) dp \right) dq. \tag{B5}$$

To evaluate the integral over p, we use Taylor expansion around q in Eq. (B5) and ϵ small. In addition, we simplify the Markovian characteristic time by taking the limit $t \to +\infty$ and neglecting the different eddy damping terms μ' and μ''. This gives the following expression for the variable viscosity term:

$$\Pi(k,t) \approx \frac{16}{15}\frac{\langle \nu'\nu'\rangle}{\nu+\kappa} k^2 E(k,t). \tag{B6}$$

Equation (B6) expresses similarly that variable viscosity terms tends to decrease the physical viscosity of the flow.

Remark that a third distant interactions approximation corresponding to $p \ll k \sim q$ should be theoretically possible although not corresponding to an interesting configuration for studying variable viscosity effects.

[1] K. Stengel, D. Oliver, and J. Booker, "Onset of convection in a variable-viscosity fluid," J. Fluid Mech. **120**, 411 (1982).
[2] M. Ogawa, G. Schubert, and A. Zebib, "Numerical simulations of three-dimensional thermal convection in a fluid with strongly temperature-dependent viscosity," J. Fluid Mech. **233**, 299 (1991).

[3] P. Tackley, "Effects of strongly variable viscosity on three-dimensional compressible convection in planetary mantles," J. Geophys. Res. **101**, 3311, doi:10.1029/95JB03211 (1996).
[4] V. Solomatov, "Scaling of temperature and stress dependent viscosity convection," Phys. Fluids **7**, 266 (1995).
[5] S. Braginskii, "Transport processes in a plasma," Rev. Plasma Phys. **1**, 205 (1965).
[6] S. Chandrasekhar, *Hydrodynamics and Hydromagnetic Stability* (Dover, 1961).
[7] J. Lindl, "Development of the indirect-drive approach to inertial confinement fusion and the target physics basis for ignition and gain," Phys. Plasmas **2**, 3933 (1995).
[8] B. Talbot, L. Danaila, and B. Renou, "Variable-viscosity mixing in the very near field of a round jet," Phys. Scr. **T155**, 014006 (2013).
[9] I. Campbell and J. Turner, "The influence of viscosity on fountains in magma chambers," J. Petrol. **27**, 1 (1986).
[10] K. Lee, S. Girimaji, and J. Kerimo, "Validity of Taylors dissipation-viscosity independence postulate in variable-viscosity turbulent fluid mixtures," Phys. Rev. Lett. **101**, 074501 (2008).
[11] G. Taylor, "Statistical theory of turbulence," Proc. R. Soc. A **151**, 421 (1935).
[12] R. Schiestel, *Modeling and Simulation of Turbulent Flows* (Wiley, 2008).
[13] R. Rubinstein, T. Clark, D. Livescu, and L.-S. Luo, "Time-dependent isotropic turbulence," J. Turbul. **5**, N11 (2004).
[14] G. K. Batchelor, "The role of big eddies in homogeneous turbulence," Proc. R. Soc. London, Ser. A **195**, 513 (1949).
[15] M. Lesieur, *Turbulence in Fluids* (Springer, 2008).
[16] J. Griffond, B.-J. Gréa, and O. Soulard, "Unstably stratified homogeneous turbulence as a tool for turbulent mixing modeling," J. Fluid Eng. (published online 2013).
[17] T. Ishida, P. A. Davidson, and Y. Kaneda, "On the decay of isotropic turbulence," J. Fluid Mech. **564**, 455 (2006).
[18] S. B. Pope, *Turbulent Flows* (Cambridge University Press, 2000).
[19] S. Orszag, "Analytical theories of turbulence," J. Fluid Mech. **41**, 363 (1970).
[20] S. Herr, L. Wang, and L. Collins, "EDQNM model of a passive scalar with a uniform mean gradient," Phys. Fluids **8**, 1588 (1996).
[21] W. Bos, H. Touil, and J. Bertoglio, "Scaling of temperature and stress dependent viscosity convection," Phys. Fluids **17**, 125108 (2005).
[22] F. Godeferd and C. Cambon, "Detailed investigation of energy transfers in homogeneous stratified turbulence," Phys. Fluids **6**, 2084 (1994).
[23] P. Sagaut and C. Cambon, *Homogeneous Turbulence Dynamics* (Cambridge University Press, 2008).
[24] M. Ulitsky and L. R. Collins, "Application of the eddy damped quasi-normal Markovian spectral transport theory to premixed turbulent flame propagation," Phys. Fluids **9**, 3410 (1997).
[25] S. Orszag, *Lectures on Statistical Theory of Turbulence* (Ecole des houches, 1974).
[26] A. Pouquet, M. Lesieur, J. André, and C. Basdevant, "Evolution of high Reynolds number two-dimensional turbulence," J. Fluid Mech. **72**, 305 (1975).
[27] C. E. Leith, "Atmospheric predictability and two-dimensional turbulence," J. Atmos. Sci. **28**, 145 (1971).
[28] M. Lesieur and D. Schertzer, "Amortissement auto similaire d'une turbulence à très grand nombre de Reynolds," J. Mech. **17**, 609 (1978).
[29] R. Kraichnan, "The structure of isotropic turbulence at very high Reynolds number," J. Fluid Mech. **5**, 497 (1959).